

## Near-Real-Time Applications of *CloudSat* Data

CRISTIAN MITRESCU, STEVEN MILLER, AND JEFFREY HAWKINS

*Naval Research Laboratory, Monterey, California*

TRISTAN L'ECUYER

*Colorado State University, Fort Collins, Colorado*

JOSEPH TURK

*Naval Research Laboratory, Monterey, California*

PHILIP PARTAIN

*Science and Technology Corporation, Fort Collins, Colorado*

GRAEME STEPHENS

*Colorado State University, Fort Collins, Colorado*

(Manuscript received 4 June 2007, in final form 28 December 2007)

### ABSTRACT

Within 2 months of its launch in April 2006 as part of the Earth Observing System A-Train satellite constellation, the National Aeronautics and Space Administration Earth System Science Pathfinder (ESSP) *CloudSat* mission began making significant contributions toward broadening the understanding of detailed cloud vertical structures around the earth. Realizing the potential benefit of *CloudSat* to both the research objectives and operational requirements of the U.S. Navy, the Naval Research Laboratory coordinated early on with the *CloudSat* Data Processing Center to receive and process first-look 94-GHz Cloud Profiling Radar datasets in near-real time (4–8 h latency), thereby making the observations more relevant to the operational community. Applications leveraging these unique data, described herein, include 1) analysis/validation of cloud structure and properties derived from conventional passive radiometers, 2) tropical cyclone vertical structure analysis, 3) support of research field programs, 4) validation of numerical weather prediction model cloud fields, and 5) quantitative precipitation estimation in light rainfall regimes.

### 1. Introduction

Understanding the life cycle and radiative, dynamic, and thermodynamic properties of global cloud cover is of paramount importance for representing clouds accurately in numerical weather prediction (NWP) and climate modeling. In light of their importance as an integral component of the hydrological cycle, coupled with a discouragingly incomplete knowledge of their feedback roles in the climate system, an increasing number

of satellite sensors dedicated to the observation of clouds have emerged. One of the newest such sensors is the 94-GHz Cloud Profiling Radar (CPR) on the *CloudSat*, second in the “A Train” satellite constellation (Stephens et al. 2002). Capable of providing the first global-scale cross sections of cloud vertical structure, *CloudSat* has collected information beneficial to a diverse assortment of fundamental research and validation efforts. The variety of sensors on the A-Train constellation offers an unprecedented opportunity to study clouds and cloud-influenced processes in the context of a well-characterized environmental state. Because *CloudSat* is the first spaceborne radar dedicated to cloud studies on global scale, it is desirable that these unique measurements be made readily available to the

---

*Corresponding author address:* Cristian Mitrescu, Naval Research Laboratory, 7 Grace Hopper Ave., MS 2, Monterey, CA 93943-5502.

E-mail: cristian.mitrescu@nrlmry.navy.mil

end user, regardless of his or her training. As it happens with new satellite sensors, the traditional form of introducing it is through near-real-time images generated using raw measurements. Given the ability of profiling clouds, the CPR complements the more traditional passive sensors currently used, thus educating the user into interpreting the full 3D cloud scene. Although certain limitations due to attenuation and multiple-scattering effects are not corrected at this early stage, it is still possible to identify certain cloud features that only such an observing system can provide. As will be shown later, *CloudSat* reveals unprecedented information about cloud layering structure, the bright band (BB) that arises as a result of melting processes, the shape/size of convective cores, presence of precipitation, and so on. The near-real-time availability of such data is also useful in picking up very interesting cases in various stages of evolution, which can be used later for both research and educational purposes.

The paper is structured as follows: Section 2 briefly describes the CPR observing capabilities. Section 3 is a short description of the concepts behind near-real-time satellite data processing. Section 4 describes the method adopted for integrating CPR datasets into the general framework of the Naval Research Laboratory (NRL) automated satellite-data-processing system, including its use in tropical cyclone (TC) monitoring and field program support. Section 5 summarizes this work.

## 2. *CloudSat's* 94-GHz observing system

As a mission sponsored by the National Aeronautics and Space Administration Earth System Science Pathfinder program, *CloudSat* targets a variety of scientific objectives related to earth science and, in particular, the complex nonlinear feedback role of clouds in the climate system (Held and Soden 2000). Launched in April of 2006 as part of the A-Train, which is a 705-km-altitude sun-synchronous polar-orbiting constellation with a ground-track repeat of 16 days, *CloudSat* has a nominal lifetime of 22 months so as to sample more than one seasonal cycle. The CPR hardware design, integrity, power consumption, and available spacecraft fuel may, however, permit extended use beyond this programmatic lifespan.

Designed to profile cloud structure, *CloudSat* features a nadir-looking 94-GHz (3 mm) radar with a minimum detectable reflectivity of approximately  $-30$  dBZ, a 70-dBZ dynamic range, and a calibration accuracy of 1.5 dBZ. With a 480-m vertical resolution (oversampled from 240-m physical "range gates") and a  $2.5 \text{ km} \times 1.4 \text{ km}$  footprint resolution, the system is well suited for sensing a wide variety of cloud systems from cirrus and

stratus to deep convective systems, with little sensitivity to the time of day or season. The measured backscatter return signal is a complicated function of cloud particle number concentration, size, shape, temperature, and phase (e.g., Heymsfield et al. 2005). With appropriate assumptions and constraints imposed, these dependencies allow the inference of basic cloud microphysical properties from measurements of radar reflectivity. However, considerable atmospheric attenuation of the radar signal at this frequency resulting from the presence of water vapor introduces additional challenges to the retrieval problem. Although it is not the emphasis of this work, we do attempt to overcome these challenges by using different atmospheric, cloud, and surface radar models in conjunction with auxiliary data as additional constraints (e.g., in physical retrievals of light rainfall).

The *CloudSat* mission also provides a unique view of the underlying surface, which exerts an important influence on the lower part of the atmosphere through frictional, turbulent, and radiative processes. Data collected by *CloudSat* will broaden our knowledge of the radiometric properties of these surfaces and may be leveraged in some cases to constrain atmospheric property retrievals such as the precipitation retrieval work mentioned previously.

The U.S. Air Force Satellite Control Network (AFSCN) located at Kirtland Air Force Base in Albuquerque, New Mexico, tracks and receives raw *CloudSat* data, does quality control on them, packages them, and sends the data to the *CloudSat* Data Processing Center (DPC) located in Fort Collins, Colorado [part of the Cooperative Institute for Research in the Atmosphere (CIRA) at Colorado State University]. The DPC is responsible for the primary and scientific data integration, processing, and distribution for the *CloudSat* program (more information was available at <http://cloudsat.cira.colostate.edu> at the time of writing). Of interest to this study are the 1B-CPR-FL and 1B-CPR products, which are essentially the same except that the latter one is rigorously checked against orbital elements that may not be available at the time at which first-look (FL) files are generated. Because of that, only the 1B-CPR-FL can be used in near-real-time applications. These radar backscatter profiles are packaged into single-orbit "granules," each of which consists of approximately 36 400 profiles that in turn each have 125 vertical bins, beginning at the first profile on or after the equator on the descending orbital node. We note that DPC posts FL images also, but only as simple quick-look images ("as is") with almost no postprocessing or geographical information on them. However, these FL images cover the entire granule as opposed to

our decision to provide near-real-time (i.e., “operational”-like) coverage over well-defined regions of the earth, as shown below.

### 3. Near-real-time satellite data processing

The Satellite Meteorological Applications Section at the NRL in Monterey, California, develops and passes on to the U.S. Navy operational centers a wide variety of applications using both satellite and NWP data. The extensive use of satellite data for monitoring weather-related events is illustrated on NRL’s public “NexSat” Internet page ([www.nrlmry.navy.mil/NEXSAT.html](http://www.nrlmry.navy.mil/NEXSAT.html); Miller et al. 2006a) and has also been demonstrated during times of conflict (Miller et al. 2006b,c). Intended for demonstrating the National Polar-Orbiting Operational Environmental Satellite System (NPOESS) capabilities, these illustrations show the potential of satellite data processing on a user-defined structured basis and the potential utility of polar-orbiting satellites for operational weather monitoring when considered as part of a large constellation of assets. With data from 33 distinct satellite sensors being received and processed on a daily basis, the NRL automated processing system not only meets the needs of the Navy for diverse and comprehensive research and development, but also provides a basis for consideration of new remote sensor retrieval algorithms. In terms of cloud remote sensing, contemporary passive satellite sensors (radiometers) are limited to statements on cloud-top properties and are for the most part unable to provide accurate information on cloud internal structure. Spaceborne active sensors, owing to their inherent profiling capabilities, are an invaluable tool for filling in the missing information and validating products derived from passive sensors.

A commonly used passive sensor for cloud property studies is the Geostationary Operational Environmental Satellite (GOES) imager. Carried on GOES-East (75°W) and GOES-West (135°W), which orbit more than 35 800 km above Earth, these images provide continuous coverage of a wide geographical area that covers the continental United States and a large portion of the Atlantic and Pacific Oceans. The GOES imager offers five moderate-band spectral channels across the optical spectrum. Whenever *CloudSat* intersects a fixed region covered by one of the GOES satellites, we overlay the vertical cross-sectional data as a way of placing the two-dimensional GOES imagery into a three-dimensional context. The reverse is also true because one can view this process as placing the two-dimensional *CloudSat* cross section into a larger spatial context. Thus, these two sensors complement each

other. In the case of a specific weather event such as tropical cyclones, we define sectors to “follow” the systems along their tracks. In this case, data used to produce imagery for these sectors can come from polar-orbiting or geostationary satellites. These images can be based either on single-channel data (i.e., data that require very little processing other than scaling) or on more complex techniques (i.e., data coming from more than one source or based on sophisticated processing algorithms). For the latter variety, data from numerical models such as the Navy Operational Global Atmospheric Prediction System (NOGAPS) are sometimes used as ancillary data for satellite-based algorithms.

In the following sections we explain the strategy adopted for integrating *CloudSat* data into our automated satellite-data-processing system for both operational and research-and-development support.

### 4. Near-real-time *CloudSat* data processing

The average data latency of CPR data is on the order of 4–8 h because of the low priority that *CloudSat* has when compared with other satellite data received at AFSCN. Although *CloudSat* holds no operational mandate, through a special agreement with DPC/CIRA we currently download the 1B-CPR-FL data within a few minutes after the raw data are received at their facility.

*CloudSat*, as a polar-orbiting satellite, provides global coverage at the expense of a much-reduced temporal coverage (for a given region). Of the approximately 15 orbits (i.e., granules) per day that *CloudSat* produces, depending on the area covered, only some will intersect one of our established satellite-monitoring sectors (stationary or fixed). Whenever that does happen, we superimpose the *CloudSat* track atop the satellite imagery (geostationary- or polar-orbiting based) for that sector and plot the corresponding radar reflectivity profile. In the following sections we describe some of the near-real-time applications that use *CloudSat* data.

#### a. First-look data processing

The premise for generating FL images was that providing a quick, near-real-time view of the vertical profile measured by the CPR would be of potential benefit to operational users (e.g., by helping them better to understand vertical structures and cloud layering, which is information that is unavailable from the operational satellite datasets). However, because some of the orbital elements as well as calibration constants may be incomplete or inaccurate in FL datasets, the FL images may contain unrealistic or incomplete data. As such, they should not be used beyond qualitative pur-

poses. Because all data contain some amount of noise, we filter the data by using a masking procedure to discriminate cloud signal from instrument noise, based on a technique described by Marchand et al. (2008). First, we compute the noise levels at highest altitudes, where only weak molecular backscatter is present and no cloud signal is anticipated, and then at all lower altitudes we compute the probabilities of exceeding such a threshold. Strong surface returns are also identified, and their locations are checked against the digital elevation map provided with the data. By adopting a  $3 \times 3$  moving window for generating the masked data, it is possible to identify clouds that have a lower detectability level than that in CPR's specifications. This, of course, is due to the additional averaging of up to nine adjacent gates. When these conditions are favorable for cloud detection, the observed minimum detectable level drops somewhere near the  $-32$ -dBZ level, thus adding to *CloudSat* sensitivity at the expense of spatial resolution. This procedure is helpful in those cases in which tenuous clouds have some appreciable horizontal and vertical extent.

In addition, temperature profiles from NOGAPS are extracted along the *CloudSat* track and overplotted on the radar reflectivity profile as contours. It provides a useful (and more commonly used and understood) thermodynamical field that gives additional meteorological context to the cloud reflectivity profile. Therefore, one can more readily identify regions that are prone to have a specific phase (i.e., a cloud-type classification), visually estimate in-cloud temperatures and possible inversions, and check for the bright band (melting layer) position, precipitation shafts, and so on.

An example of the CPR quick-look radar profile is presented in Fig. 1. Collected on 21 January 2007 by GOES-East, it shows an area centered at  $65^\circ\text{W}$  that covers the western Atlantic Ocean and the eastern part of the United States (the "NW Atlantic" overview sector of NexSat). On the right side of the image is a fast-moving cold front crossed by *CloudSat*. Behind it, cellular cloud structure (stratocumulus and cumulus, indicated on the figure by Sc/Cu) in the cold sector of the system is clearly visible as northwesterly winds advance over warmer waters of the northern Gulf Stream. However, not visible from the GOES image is cloud vertical structure, as revealed by *CloudSat*. Figure 1 illustrates cloud structure changes as one moves northward through the cold front: starting from elevated cirrus to strong, wide convective cloud systems followed by clusters of shallower convective clouds. Cloud tops and their layering structure are clearly visible. Also, as indicated on the figure, the melting layer or BB close to the  $0^\circ\text{C}$  isotherm is identifiable. Such a BB indicates the

presence of both ice and liquid phase in the cloud, with precipitation likely below. On occasion, strong convective cores are also clearly depicted by *CloudSat* but not by the GOES image. Local and mesoscale vertical features are visible. Overall, the CPR provides a novel view of cloud vertical structure that complements the 2D structure provided by the passive sensor. The red line shows the *CloudSat* satellite ground track. To facilitate cross-referencing with the GOES image, the black dots overlaid on the ground track represent 1 min of orbit time. The "start" and "end" labels identify the UTC times at which *CloudSat* enters and exits this geographical area. Below the GOES image, we display radar profiles from start to end. Depending on the length of the track within the sector, one, two, or more subpanels will be displayed. Navigational elements are also displayed: latitude, longitude, and UTC time corresponding to each minute of flying. A north or south arrow indicates whether the current pass is on an ascending or descending orbit. The measured radar reflectivity profile is presented using a color bar that ranges from  $-30$  to  $+20$  dBZ. Altitude and pressure are shown on the left and right ordinate axes. A horizontal scale bar is drawn next to the reflectivity color bar. The corresponding 3-hourly interpolated profile of air temperature from NOGAPS is also displayed as contours. Each image file has an identification structure within its naming convention that carries information about the date and time of the satellite pass, the corresponding sector (or name of TC storm for a moving sector), the field that is being plotted, and which satellite data were used for producing it. For these files, the extension "FL" is also used. As the calibrated and better geolocated 1B-CPR files are processed (usually after a 1-week delay), these FL files are replaced, as indicated by an "x" in the naming structure. However, because the same routine is applied to these new data, the images have the same general appearance and labeling as the FL versions. Only when orbital elements and/or calibration constants differ significantly will the reflectivity field appear notably different.

The average processing time for one full orbit granule is about 2 min for masking and 1 min for numerical model data extraction on a 2.66-GHz dual-processor computer. After that, one sector image is produced in about 10 s. We currently process multiple fixed sectors around the world and a variable number of moving sectors tracking TC systems. The projection type and characteristics (i.e., center latitude and longitude and horizontal dimensions and resolution) of fixed sectors are unchanged, whereas the sectors for TC systems have dynamic characteristics. The automated processing takes into account all of these parameters for an

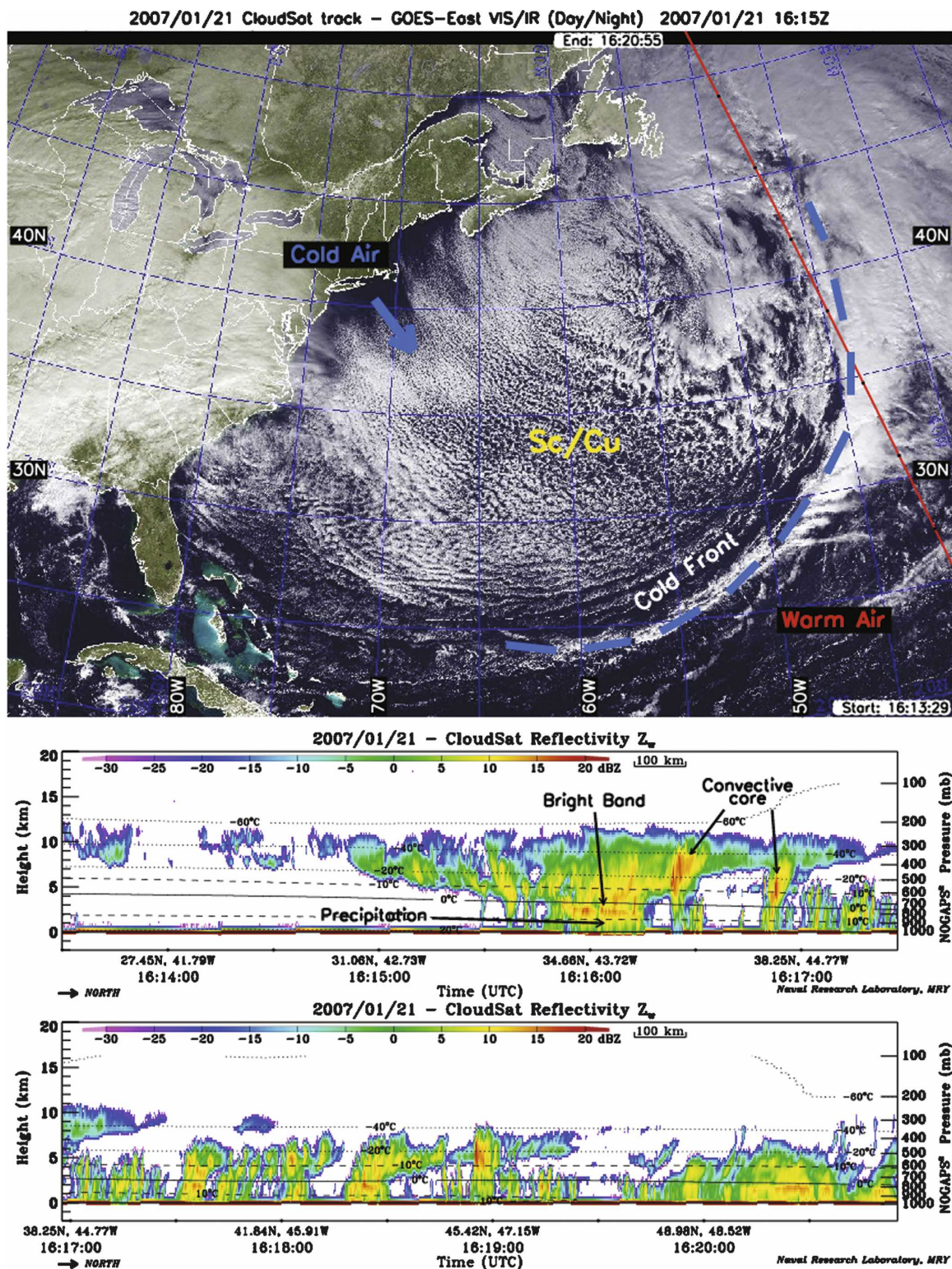


FIG. 1. Example of GOES data and the corresponding *CloudSat* radar profile for the northwestern Atlantic sector at 1615 UTC 21 Jan 2007.



accurate representation. We also added the option of reading latitude and longitude files for the cases in which a more complicated projection is used or data are so structured.

Because we provide satellite support for various missions and demonstrations, we added the option of displaying other vector graphics of interest (site locations, target area, etc.) that help in rapid identification of various elements relevant to decision making.

#### *b. CloudSat processing for the tropical cyclone Internet page*

*CloudSat*'s sensitivity to cloud droplets has proven very useful in profiling one of the most severe weather phenomena on Earth: tropical cyclones. Because of frequent upper-level clouds, all passive visible/IR sensors are severely limited in monitoring these large and powerful systems that contain high winds and heavy precipitation. Because these storms develop over warm tropical ocean waters, where in situ observations are scarce, satellite remote sensing is a superb tool for observing and monitoring their temporal and spatial evolution. However, their vertical structure is not resolved by optical-spectrum passive instruments because of rapid attenuation by cloud liquid water. Although multispectral observations at microwave wavelengths can depict a cloud's pseudovertical structure, because of the dependency of the optical depth on frequency, its real-time application is somewhat limited to a reduced number of highly specialized/trained end users. Radars, on the other hand, can penetrate deep into the dense cloud/precipitation structure before being totally attenuated, providing a better-understood vertical slice of TC structure.

The TC Internet (Worldwide Web) page's near-real-time processing is driven by the 6-hourly updates provided by the Joint Typhoon Warning Center (JTWC; Pearl Harbor, Hawaii), the Central Pacific Hurricane Center (CPHC; Hawaii), and the National Hurricane Center (NHC; Miami, Florida). These three operational agencies are responsible for monitoring and warning on all areas around the world susceptible to TCs. JTWC, CPHC, and NHC use all available information (satellites, surface observations, upper-air balloons, commercial and TC aircraft reports, and NWP analyses and forecasts) to provide warnings on all active TCs and those systems that show the most likelihood to evolve into TCs. The updated storm positions (lat/lon) from JTWC/CPHC/NHC are sent automatically to NRL via the Automated Tropical Cyclone Forecasting system (Sampson and Schrader 2000). Existing TCs are thus updated and the storm-centered products are shifted accordingly, and "new" storms are

then initiated into the automated processing stream. The full suite of geostationary and polar-orbiter digital datasets is then interrogated to see which newly arriving data will be processed to create new products. If the storm is new, then the last 24 h of passive microwave products and the last 4 h of geostationary data are reprocessed within minutes and posted to the TC Internet page (Hawkins et al. 2001).

*CloudSat* data are processed as soon as they are received at NRL from the DPC, typically within 4–8 h of being observed. New *CloudSat* data are checked to determine whether they cover any existing TC sector and are then processed into five potential products that overlay the *CloudSat* radar profiles on nearly time coincident *Aqua* satellite sensors: Moderate Resolution Imaging Spectroradiometer (MODIS) visible (VIS) and IR, Advanced Microwave Scanning Radiometer for Earth Observing System (AMSR-E) 89-GHz horizontal-polarization imagery, and VIS/IR data from the geostationary satellite with the best TC view angle. Although the radar profile is identical on each of these images, these products provide the satellite analyst with enhanced information content on the 2D cloud structure. During the 2006 TC season, *CloudSat* had more than 900 TC crossings, and, through the synthesis with spatial images, in some cases it has provided unique views of TC inner-core cloud and precipitation structure.

The first example we illustrate is that of Hurricane Ileana, which started as a tropical depression south-southwest of Acapulco, Mexico, and gradually strengthened to hurricane status on 22 August 2006, followed by a rapid intensification to a major hurricane. Figure 2 highlights a *CloudSat* overpass of Hurricane Ileana (maximum sustained wind of  $54 \text{ m s}^{-1}$ ) at 2100 UTC 23 August 2006 that reveals a complex horizontal and vertical structure. The top part of the image shows the 2D horizontal cloud distribution as captured by the *Aqua* MODIS visible sensor at 1-km resolution, with the *CloudSat* track superimposed in red (dots denote 15-s flight track intervals), and the bottom part depicts the CPR's vertical profile. The cloud tops created by the vigorous convective activity reach about 16 km and span more than 800 km, with spiraling bands clearly visible. The *CloudSat* vertical cross section provides a wealth of information: 1) upward sloping of cloud tops toward the TC eye or storm center, 2) a rain-free region associated with both the eye and a moatlake region to the south located between the inner eyewall and an outer rain band, 3) ready identification of intense rain areas along the radar's nadir-only ground track, 4) cloud-base measurements to the south as the cirrus cloud bases get progressively higher away from the con-

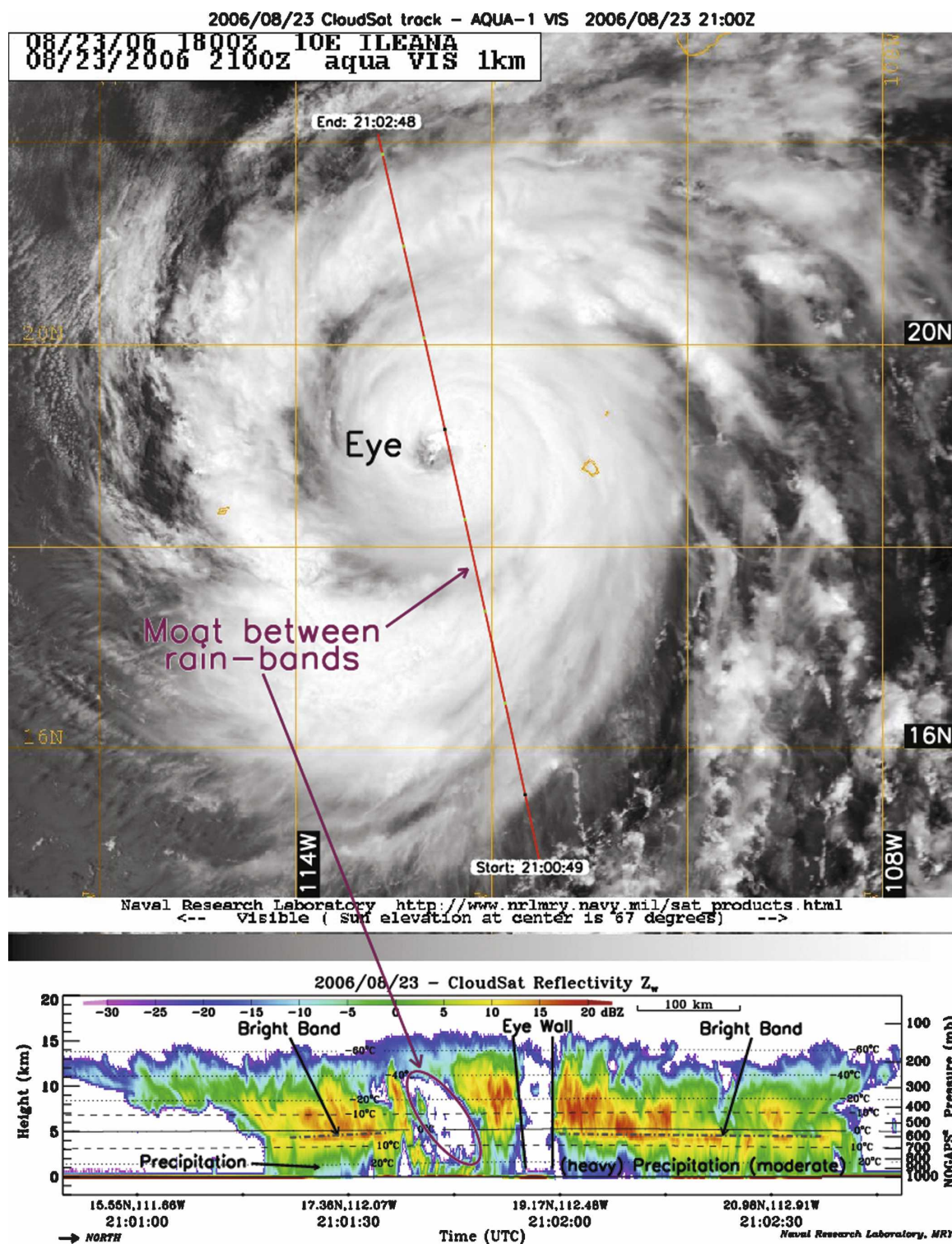


FIG. 2. The A-Train (*Aqua*-VIS and *CloudSat*) view of Hurricane Ileana at 2100 UTC 23 Aug 2006. See text for explanations.

vective source region, and 5) mapping of the upward sloping BB, an indication of a melting layer. Monitoring cloud-top-height changes and, more important, the vertical extent of precipitation is crucial to understanding TC structure/intensity. *CloudSat* and the Tropical Rainfall Measuring Mission (TRMM) precipitation radar (PR) work together to provide vital 3D details. Knowledge of rain-free areas is essential to monitoring the latent heat of condensation produced within the storm's inner core. The NOGAPS 3D thermal structure is included as isotherms within Fig. 2, and we have found that the 0°C isotherm typically matches well with the height of the BB. In many cases, the strong attenuation of cloud and especially precipitation can completely attenuate the radar signal before reaching the surface. Ileana then underwent an eyewall replacement cycle. Although such an event is usually followed by a strengthening, because of its movement over cooler ocean waters the storm continued to weaken, until it was downgraded to a tropical depression 4 days later.

Another illustrative example is a *CloudSat* overpass of western Pacific Typhoon Durian at 0210 UTC 7 September 2006 while the storm was at an estimated wind intensity of approximately  $40 \text{ m s}^{-1}$  (see Fig. 3). Here, Durian is caught in a highly explosive stage (after reaching its maximum intensity earlier) that highlights the value of *CloudSat*'s unique profiling capabilities. The *Aqua* MODIS IR imagery includes a massive cirrus canopy but does not permit the analyst to ascertain much information pertaining to the organization of rainbands or the storm structure beneath it. However, *CloudSat* details a small but explosive convective region that is responsible for the mushroomlike cloud appearance that spans over 180 km around it. Huge convectively active regions like this one are called "hot towers" and are one of the mechanisms that create and sustain the TC warm core. In addition, hot towers have been postulated to be associated with rapid TC intensification (Montgomery et al. 2006; Schubert and Hack 1982). In fact, Durian did intensify shortly after this particular convective burst event. Similar hot towers can be viewed by the TRMM PR because the precipitation signature is so large and involves very large droplets. Note that Fig. 3 also detects low and midlevel cloud and rain structures both north and south of the convective cells that are extremely difficult to extract from the IR image alone. When 1B-CPR calibrated data become available, the above near-real-time process is repeated for consistency and all *CloudSat* images are posted on the NRL TC page ([www.nrlmry.navy.mil/tc\\_pages/TC.html](http://www.nrlmry.navy.mil/tc_pages/TC.html)) that contains a "one-stop-shop" of up-to-date storm-centered satellite products for global TCs (Hawkins et al. 2001). In addition to images, data

extraction is also done along the CPR tracks for all TC crosses, thus creating a comprehensive database (which at the time of writing could be accessed at [www.nrlmry.navy.mil/archdat/tropical\\_cyclones/CPR\\_TC\\_Intercepts](http://www.nrlmry.navy.mil/archdat/tropical_cyclones/CPR_TC_Intercepts)). Based on TC geolocation, it contains radial information along *CloudSat* track about CPR reflectivity, AMSR-E brightness temperature and derived products (wind, SST, precipitation, liquid water path, and humidity), and NOGAPS data fields. By capturing different stages in TC evolution, it provides an invaluable tool for research purposes.

### c. Near-real-time support for field programs

Although validation is an important utility of the *CloudSat* dataset, it is recognized that *CloudSat* itself must be validated. Intensive field campaigns aimed at gathering as much in situ data from as many complementary/redundant instruments as possible over a target area during a limited time range are desired. These data are useful in evaluating satellite sensor calibration and the fidelity of environmental property retrieval algorithms applied to the satellite observations.

The Canadian *CloudSat/Cloud-Aerosol Lidar and Infrared Pathfinder Satellite Observation (CALIPSO)* Validation Project (C3VP) experiment ([www.c3vp.org](http://www.c3vp.org)), for example, sought to collect datasets to evaluate cloud, precipitation, and aerosol products from *CloudSat* and *CALIPSO* associated with cold-season weather systems in the Great Lakes region of Canada. During four intensive observing periods (IOPs) spanning autumn 2006 and winter 2006/07, more than 25 coordinated flights were made under the A-Train and over ground-based instrumentation at the Centre for Atmospheric Radiation Experiments (CARE) facility in south-central Ontario, Canada. The experiment yielded several high-quality datasets from ground-based and airborne X-, C-, W-, Ka-, and Ku-band radar; in situ observations of cloud particle size distributions, water contents, and precipitation rates; and a suite of passive remote sensing instruments. These measurements, often collocated with satellite overpasses, cover a wide range of cold-season cloud systems featuring light rainfall, snowfall, and multilayer and mixed-phase clouds. Although the experiment concluded very recently, these datasets are already proving to be an invaluable resource for the developers of cloud and precipitation algorithms for *CloudSat*.

An example of data collected over a target area for aircraft flights along the CPR ground track is presented in Fig. 4. The targeted area is denoted by a thick blue line. The CARE facility location (outside the displayable area for this case) and Ottawa (where aircraft are stationed) are also identified. NexSat imagery (in-



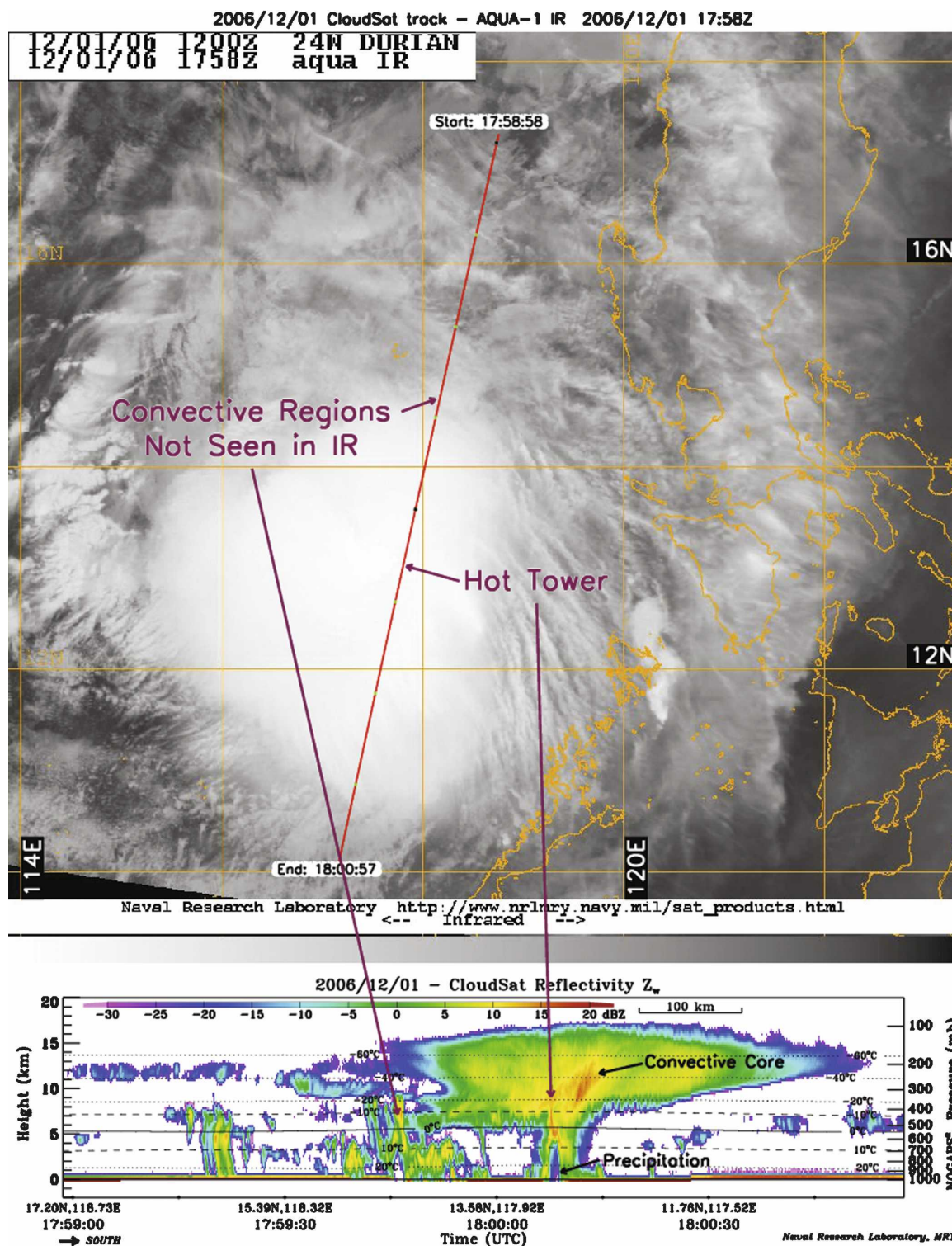


FIG. 3. The A-Train (*Aqua*-IR and *CloudSat*) view of Typhoon Durian at 1800 UTC 1 Dec 2006. See text for explanations.

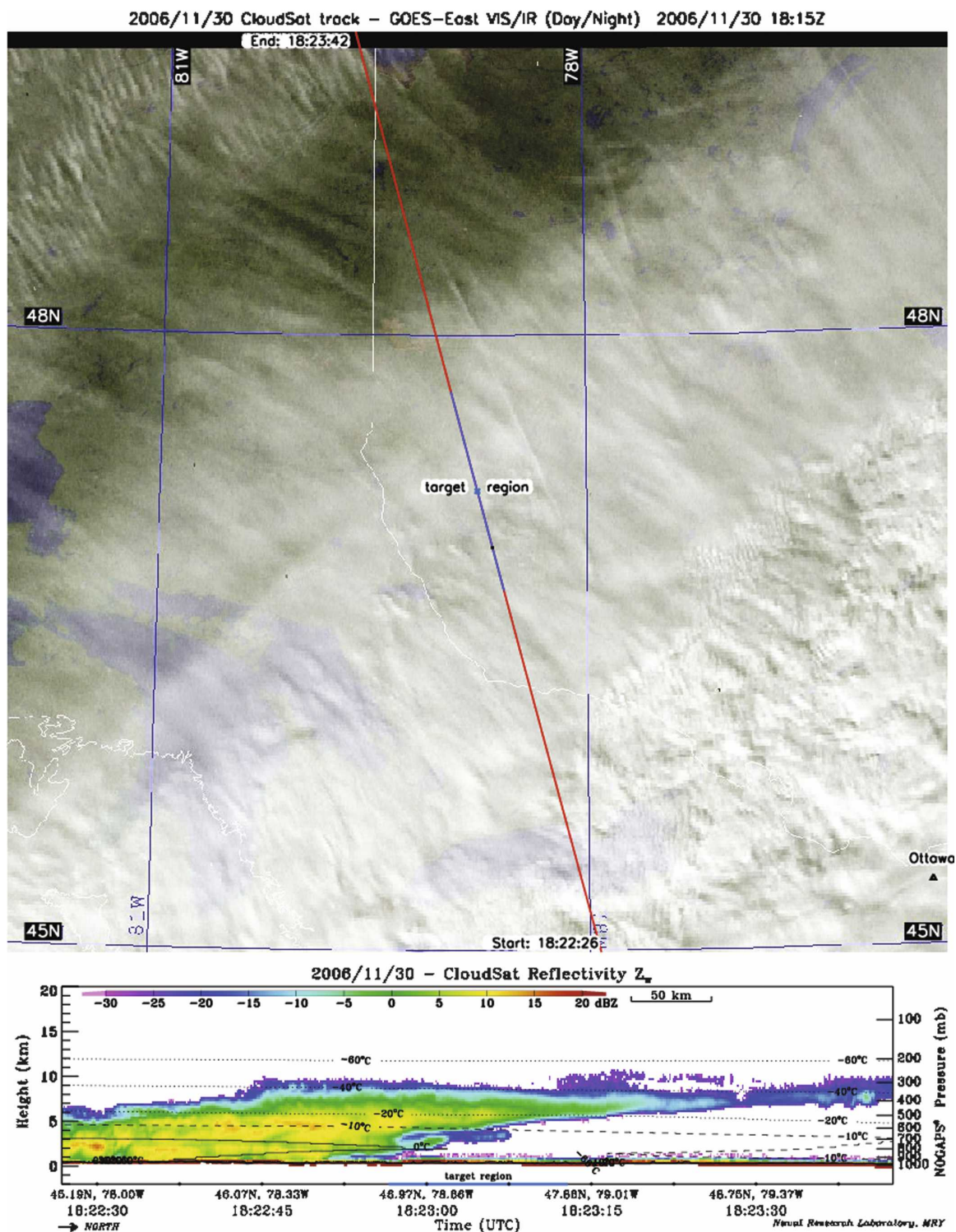


FIG. 4. GOES and *CloudSat* supporting the C3VP experiment. The validation region is identified as “target region” in both panels. See text for more details.



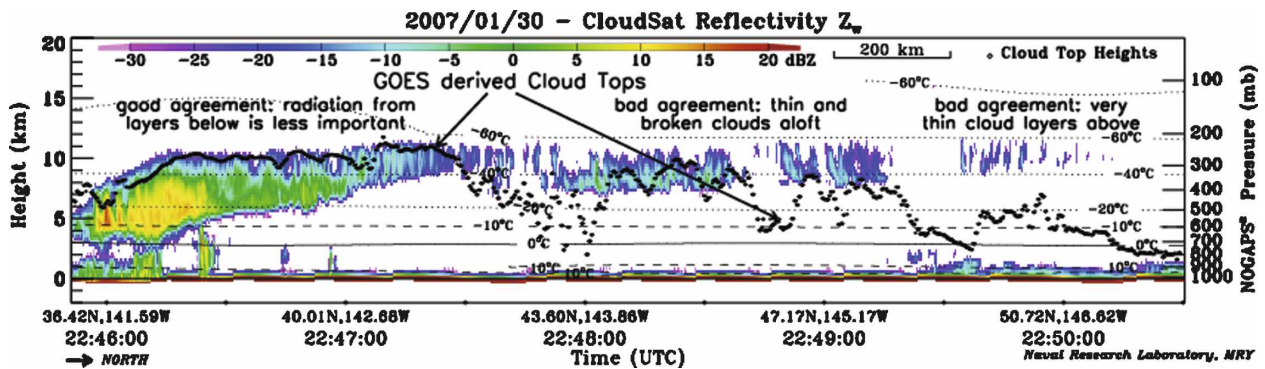


FIG. 5. GOES-derived cloud-top heights vs *CloudSat*'s vertical profile for a sector over the northeastern Pacific at 2248 UTC 30 Jan 2007.

cluding near-real-time GOES, MODIS, and *CloudSat* products) supported the C3VP science team's efforts to coordinate aircraft and surface measurements with A-Train overpasses in the context of dynamic environmental conditions and cloud cover. The combination of this diverse array of products provides a simultaneous glimpse at the detailed vertical structure of the scene and its broader meteorological context that is critical for flight planning and decision making for any kind of field experiment.

Additional field campaigns, such as the Tropical Composition, Clouds, and Climate Coupling Experiment (TC4) that took place off the coast of Panama in July and August 2007, will leverage NexSat products in a similar way. TC4 was dedicated to addressing important science questions about the connection between convection and trace gases/cirrus clouds in the upper atmosphere and providing additional high-quality datasets for evaluating A-Train data products, making it an ideal application for the near-real-time products generated at NRL.

Taking advantage of *CloudSat*'s ability to range-resolve cloud top and base, we have also started a near-real-time comparison (posted on NexSat) between our passive sensor (GOES)-derived cloud top heights, which use a three-channel retrieval approach (Mitrescu et al. 2006), and those detected by the CPR. Figure 5, showing a cross section through a fast-moving frontal system over the northeastern Pacific at 2250 UTC 30 January 2007, provides a good example of how *CloudSat* can reveal caveats to our passive-retrieval approaches. Three distinct regions are identifiable. In the first (on the left-hand side of Fig. 5), the passive sensor's cloud-top-height algorithm does a relatively good job in assigning a correct top altitude because the simplified model closely matches the observed clouds. As the cloud becomes more transparent (because of the

decrease in both geometrical thickness and reflectivity, as seen in the midsection of the figure), errors in retrieved optical depth manifest as increasing differences between GOES- and CPR-retrieved cloud-top heights. The disagreement is most pronounced when the cloud vertical structure as seen by CPR shows a multilayer structure that contradicts the model assumption of one-layer cloud (right-hand side of the figure). These comparisons will help us in correcting, accounting for errors in, and understanding limitations of the physical cloud model used for GOES-based height retrievals, thereby leading to improvement in the retrieval of other microphysical and optical parameters. Moreover, qualitative comparisons between the *CloudSat* reflectivity field and other passive-sensor output can be made. As such, some of the *CloudSat* derived products that are available through DPC/CIRA such as cloud class, liquid and ice water content, and precipitation rates can also be compared with numerical model output and/or other satellite-based techniques. However, all of these efforts are currently works in progress and therefore will be discussed in more detail sometime in the future.

## 5. Summary and conclusions

Designed for profiling the vertical structure of clouds, *CloudSat*'s 94-GHz CPR adds a third dimension of information needed for assessing the influences and feedbacks that clouds exert on the climate system. Placed in a sun-synchronous orbit as part of the A-Train constellation of satellites, it provides a vertical cross section of cloud structures on a global scale. Although most of the thin cirrus clouds are not being detected by this active sensor (as indicated by preliminary comparisons with *CALIPSO* lidar), it provides invaluable information for all other cloud types, especially those that are precipitating and are directly re-

sponsible for the intensity and distribution of precipitation and moisture and all related effects that influence the evolution of weather on many temporal and spatial scales.

Although *CloudSat* is a research satellite, this work offers a glimpse into the near-real-time use of *CloudSat* data in combination with the more widely used (and perhaps better understood) data from passive sensors. Through the courtesy of our colleagues at DPC who provide us with up-to-the-minute *CloudSat* data, we have developed a near-real-time processing and distribution of *CloudSat* data for both research and quasi-operational use. Presented here are some applications that combine passive data from sensors on geostationary [like GOES, Meteosat, or the Geostationary Meteorological Satellite (GMS)/Multifunctional Transport Satellite (MTSAT)] or polar-orbiting satellites (such as *Aqua*) that only have limited ability to characterize cloud vertical structures with the active *CloudSat* sensor that by design resolves such a structure. Despite the very narrow area covered by this CPR sensor, since its launch *CloudSat* has provided the scientific community with unique views (and details) of the most powerful weather events: the tropical cyclones. Although we only presented two such cases, *CloudSat* data, along with other remote sensor data, are being collected for a closer inspection. Within the bounds of sensitivity, CPR profiles provide detailed cloud structure/content information that is extremely useful for validating cloud-resolving-model simulations and other remote sensing techniques. Support provided for the C3VP experiment and validation for the GOES-derived cloud-top-height algorithm represent just some applications illustrated here.

We are currently only in the very early stages of processing and understanding the data provided by the *CloudSat* CPR sensor. Our current efforts are focused on development of accurate forward models for the CPR that account for all relevant effects that influence our ability to retrieve correctly the cloud microphysical state vector. We therefore move from the operational mode into research-and-development mode, aimed at improving our understanding of cloud structure and, ultimately, cloud-related feedbacks. The visualization-based approach described in this paper is useful for identifying not only good case studies but also potential deficiencies in the observing system. The NexSat and TC demonstration-Internet-page packages are ideal tools for the qualitative communication of *CloudSat* capabilities. The combination of sensors described above permits us to seek model improvements in deficient (or nonexistent) areas like the addition of multiple-

scattering effects, surface return characterization, and brightband model description. In the future, we seek the addition of new operational products not only from the *CloudSat* sensor, but also from other sensors on the A-Train (e.g., Mitrescu et al. 2005) that can be used for deriving new products such as precipitation, particle number concentration and characteristic diameter, cloud type, model validation/characterization, and so on.

It is also important to note the educational benefits of *CloudSat*. One of the primary uses of *CloudSat* will be in meteorological training and education. Data displays are often so intuitive that even younger students can benefit. Online tutorials are being developed by the Global Learning and Observation to Benefit the Environment (GLOBE) program ([www.globe.gov/globe\\_flash.html](http://www.globe.gov/globe_flash.html)). *CloudSat* has been featured on a Public Broadcast Service television program. Educational case examples are available at the NRL NexSat Internet site mentioned earlier (see the headlines link), and training will likely become available from the Cooperative Program for Operational Meteorology, Education and Training (COMET; [www.comet.ucar.edu](http://www.comet.ucar.edu)). We thus see our efforts being integrated into a more general framework.

**Acknowledgments.** The support of our research sponsors the Office of Naval Research, under Program Element PE-0602435N, is gratefully acknowledged. We also thank Mr. K. Richardson (NRL) and Dr. R. Wade (SAIC) for providing auxiliary data and archival services, Mr. T. Lee (NRL) for liaisons with the COMET program, and Ms. N. Tourville (Colorado State University) for her assistance in constructing the *CloudSat* tropical cyclone cross sections database. We thank the other members at the NRL TC Worldwide Web team: Mr. C. Sampson (NRL) and Mr. J. Kent (SAIC).

## REFERENCES

- Hawkins, J. D., T. F. Lee, J. Turk, C. Sampson, J. E. Kent, and K. Richardson, 2001: Real-time Internet distribution of satellite products for tropical cyclone reconnaissance. *Bull. Amer. Meteor. Soc.*, **82**, 567–578.
- Held, I. M., and B. J. Soden, 2000: Water vapor feedback and global warming. *Annu. Rev. Energy Environ.*, **25**, 441–475.
- Heymsfield, A. J., Z. Wang, and S. Matrosov, 2005: Improved radar ice water content retrieval algorithms using coincident microphysical and radar measurements. *J. Appl. Meteor.*, **44**, 1391–1412.
- Marchand, R. T., G. Mace, T. Ackerman, and G. L. Stephens, 2008: Hydrometeor detection using *Cloudsat*—An earth-orbiting 94-GHz cloud radar. *J. Atmos. Oceanic Technol.*, **25**, 519–533.
- Miller, S. D., and Coauthors, 2006a: NexSat: Previewing NPOESS/VIIRS imagery capabilities. *Bull. Amer. Meteor. Soc.*, **87**, 433–446.



- , J. D. Hawkins, T. F. Lee, F. J. Turk, and K. Richardson, 2006b: MODIS views of Operation Iraqi Freedom in collage. *Int. J. Remote Sens.*, **27**, 1279–1284.
- , and Coauthors, 2006c: MODIS provides a satellite focus on Operation Iraqi Freedom. *Int. J. Remote Sens.*, **27**, 1285–1296.
- Mitrescu, C., J. M. Haynes, G. L. Stephens, S. D. Miller, G. M. Heymsfield, and M. J. McGill, 2005: Cirrus cloud optical, microphysical and radiative properties observed during the CRYSTAL-FACE experiment: A lidar-radar retrieval system. *J. Geophys. Res.*, **110**, D09208, doi:10.1029/2004JD005605.
- , S. D. Miller, and R. H. Wade, 2006: Cloud optical and microphysical properties derived from satellite data. Preprints, *14th Conf. on Satellite Meteorology and Oceanography*, Atlanta, GA, Amer. Meteor. Soc., P1.7. [Available online at <http://ams.confex.com/ams/pdfpapers/100515.pdf>.]
- Montgomery, M. T., M. E. Nicholls, T. A. Cram, and A. B. Saunders, 2006: A vortical hot tower route to tropical cyclogenesis. *J. Atmos. Sci.*, **63**, 355–386.
- Sampson, C. R., and A. J. Schrader, 2000: The automated tropical cyclone forecasting system (version 3.2). *Bull. Amer. Meteor. Soc.*, **81**, 1231–1240.
- Schubert, W. H., and J. J. Hack, 1982: Inertial stability and tropical cyclone development. *J. Atmos. Sci.*, **39**, 1687–1697.
- Stephens, G. L., and Coauthors, 2002: The *CloudSat* mission and the A-Train: A new dimension of space-based observations of clouds and precipitation. *Bull. Amer. Meteor. Soc.*, **83**, 1771–1790.